

Hopfield neural network-based image restoration with adaptive mixed-norm regularization

Yuannan Xu (许元男), Liping Liu (刘丽萍), Yuan Zhao (赵远),
Chenfei Jin (靳辰飞), and Xiudong Sun (孙秀冬)*

Department of Physics, Harbin Institute of Technology, Harbin 150001, China

*E-mail: xdsun@hit.edu.cn

Received December 3, 2008

To overcome the shortcomings of traditional image restoration model and total variation image restoration model, we propose a novel Hopfield neural network-based image restoration algorithm with adaptive mixed-norm regularization. The new error function of image restoration combines the L_2 -norm and L_1 -norm regularization types. A method of calculating the adaptive scale control parameter is introduced. Experimental results demonstrate that the proposed algorithm is better than other algorithms with single norm regularization in the improvement of signal-to-noise ratio (ISNR) and vision effect.

OCIS codes: 100.3020, 100.3190, 200.4260.

doi: 10.3788/COL20090708.0686.

Image restoration deals with the recovery of an original scene from its degraded image^[1-3]. Since neural network-based image restoration does not generate ringing effect which relates to matrix inversion for solving Euler-Lagrange equation, it can restore a higher quality image. Most neural network-based image restoration algorithms use L_2 -norm as regularization item and an isotropic regularizing operator such as Laplace operator^[4-10]. We call it traditional image restoration model here. Although this type of regularization based on L_2 -norm and Laplace operator has a good ability to smooth and remove noise, it blurs the edges of restored image more or less and the vision effect is not very good. To preserve edges, a total variation-based image restoration model is proposed^[11-15]. However, the model is mainly suitable for the images with smooth patch and evident edge. By experiments, we find that the restored image appears ladder effect when image dissatisfy this condition, for example, the change of slope edge is slow. Sometimes, noise can be wrongly considered as false edge. To overcome these shortcomings of the two image restoration models, we propose a novel Hopfield neural network-based image restoration algorithm using adaptive mixed-norm regularization.

The image degradation model in a matrix operation can be expressed as

$$\mathbf{g} = H\mathbf{f} + \mathbf{n}, \quad (1)$$

where \mathbf{g} , \mathbf{f} , and \mathbf{n} are vectors corresponding to the lexicographically organized degraded image, original image, and additive noise, respectively, H is the blur matrix corresponding to a point spread function (PSF). For the case of a convolution system, H usually takes the form of a block Toeplitz matrix. Commonly, image restoration is to minimize an error measurement such as the constrained squared error function:

$$E = \frac{1}{2} \|\mathbf{g} - H\mathbf{f}\|_2^2 + \frac{1}{2} \lambda \left\| D\hat{\mathbf{f}} \right\|_2^2, \quad (2)$$

where $\|\cdot\|_2$ is L_2 norm, $\hat{\mathbf{f}}$ is the restored image estimate

vector, λ is the regularizing parameter, \mathbf{D} is a block Toeplitz matrix generated by the regularizing operator. In this image restoration model, the regularizing operator is a Laplace operator, which can be written as^[16]

$$d_{\text{Laplace}} = \frac{1}{8} \begin{bmatrix} 0 & 1 & 0 \\ 1 & -4 & 1 \\ 0 & 1 & 0 \end{bmatrix}. \quad (3)$$

The error function based on total variation is given by

$$E = \frac{1}{2} \|\mathbf{g} - H\mathbf{f}\|_2^2 + \frac{1}{2} \lambda \left\| \nabla \hat{\mathbf{f}} \right\|_1, \quad (4)$$

where $\|\cdot\|_1$ is L_1 norm, ∇ is the gradient operator, $|\nabla \mathbf{f}| = \sqrt{(\partial \mathbf{f} / \partial x)^2 + (\partial \mathbf{f} / \partial y)^2}$. In this image restoration model, the action of smoothing filter is not imposed so that the edge information can be preserved.

For obtaining a better solution to the image restoration, we propose to combine the benefits of the traditional model and total variation model. To fit Hopfield neural network based processing, a novel error function with mixed-norm regularization is proposed:

$$E = \frac{1}{2} \|\mathbf{g} - H\mathbf{f}\|_2^2 + \frac{1}{2} \lambda \eta \left\| D\hat{\mathbf{f}} \right\|_2^2 + \frac{1}{2} \lambda (1 - \eta) \left\| \nabla \hat{\mathbf{f}} \right\|_1, \quad (5)$$

where η is a regularizing scale control parameter and its span is $[0, 1]$. The image restoration model with mixed-norm regularization is aimed to overcome the shortcomings and keep the advantages of the two above-mentioned models. Blurring of image detail, false edge, and ladder effect can be removed to a certain extent, and a better image restoration effect can be achieved.

Hopfield neural network method is designed to minimize a quadratic programming problem. The energy function of Hopfield neural network has the following form:

$$E_{\text{HNN}} = -\frac{1}{2} \hat{\mathbf{f}}^T W \hat{\mathbf{f}} - b^T \hat{\mathbf{f}} + c, \quad (6)$$

where W is the interconnection weight matrix and the (i, j) th element of W corresponds to the interconnection

strength between neurons (pixels) i and j in the network, the term c is a constant term of the energy function. The vector \mathbf{b} corresponds to the bias input to each neuron. The discrete form can be written as

$$E_{\text{HNN}} = -\frac{1}{2} \sum_{i=1}^L \sum_{j=1}^L w_{ij} \hat{f}_i \hat{f}_j - \sum_{i=1}^L b_i \hat{f}_i + c, \quad (7)$$

where w_{ij} is the interconnection weight between pixels i and j , b_i is the bias input to neuron (pixel) i , and the image size is $M \times N$, $L = MN$.

For combining the total variation regularization and the energy function of Hopfield neural network, the non-linear gradient operator is decomposed to the sum of linear operators. An approximation is proposed as

$$|\nabla f| \approx |\partial f / \partial x| + |\partial f / \partial y|. \quad (8)$$

The gradient operators in four directions can be written as

$$d_E = \begin{bmatrix} 0 & 0 & 0 \\ 0 & -1 & 1 \\ 0 & 0 & 0 \end{bmatrix}, d_W = \begin{bmatrix} 0 & 0 & 0 \\ 1 & -1 & 0 \\ 0 & 0 & 0 \end{bmatrix}, \\ d_N = \begin{bmatrix} 0 & 1 & 0 \\ 0 & -1 & 0 \\ 0 & 0 & 0 \end{bmatrix}, d_S = \begin{bmatrix} 0 & 0 & 0 \\ 0 & -1 & 0 \\ 0 & 1 & 0 \end{bmatrix}. \quad (9)$$

The discrete form of error function can be written as

$$E = \frac{1}{2} \sum_{p=1}^L \left(g_p - \sum_{i=1}^L h_{pi} \hat{f}_i \right)^2 + \frac{1}{2} \lambda \eta \sum_{p=1}^L \left(\sum_{i=1}^L d_{pi} \hat{f}_i \right)^2 \\ + \frac{1}{2} \lambda (1 - \eta) \sum_{p=1}^L \left(\left| \sum_{i=1}^L d_{E,pi} \hat{f}_i \right| + \left| \sum_{i=1}^L d_{W,pi} \hat{f}_i \right| \right. \\ \left. + \left| \sum_{i=1}^L d_{N,pi} \hat{f}_i \right| + \left| \sum_{i=1}^L d_{S,pi} \hat{f}_i \right| \right), \quad (10)$$

where h and d are the elements of the matrices H and D , respectively. Equation (10) is transformed to be

$$E = \frac{1}{2} \sum_{i=1}^L \sum_{j=1}^L \left(\sum_{p=1}^L h_{pi} h_{pj} + \lambda \eta \sum_{p=1}^L d_{pi} d_{pj} \right) \hat{f}_i \hat{f}_j \\ - \sum_{i=1}^L \left(\sum_{p=1}^L g_p h_{pi} - \frac{1}{2} \lambda (1 - \eta) \sum_{p=1}^L \right. \\ \left. (G_{E,p} d_{E,pi} + G_{W,p} d_{W,pi} + G_{N,p} d_{N,pi} + G_{S,p} d_{S,pi}) \right) \hat{f}_i \\ + \frac{1}{2} \sum_{p=1}^L (g_p^2). \quad (11)$$

where $G_{E,p} = \text{sign} \left(\sum_{i=1}^L d_{E,pi} \hat{f}_i \right)$, $G_{W,p} = \text{sign} \left(\sum_{i=1}^L d_{W,pi} \hat{f}_i \right)$, $G_{N,p} = \text{sign} \left(\sum_{i=1}^L d_{N,pi} \hat{f}_i \right)$, $G_{S,p} = \text{sign} \left(\sum_{i=1}^L d_{S,pi} \hat{f}_i \right)$, $\text{sign}(\cdot)$ is a sign function.

Comparing Eq. (7) with the corresponding Eq. (11), the interconnection weights w_{ij} and bias inputs b_i are shown to be

$$w_{ij} = - \sum_{p=1}^L h_{pi} h_{pj} - \lambda \eta \sum_{p=1}^L d_{pi} d_{pj}, \\ b_i = \sum_{p=1}^L g_p h_{pi} - \frac{1}{2} \lambda (1 - \eta) \sum_{p=1}^L (G_{E,p} d_{E,pi} \\ + G_{W,p} d_{W,pi} + G_{N,p} d_{N,pi} + G_{S,p} d_{S,pi}). \quad (12)$$

When $\eta = 1$, the mixed-norm model transforms to the traditional model. When $\eta = 0$, the mixed-norm model transforms to the total variation model.

We hope the values of scale control parameter η should be determined adaptively using the local characteristic of each pixel, and η is a larger value for the smooth or flat areas, a smaller value for the edge or texture regions, and an intermediate value for slope edge to reduce ladder effect. We propose the following method to calculate the adaptive η value.

$$A_{\text{in}} = \max(0, (\sigma_{\text{in}} - \sigma_{\text{n}})), \quad (13)$$

$$A_{\text{out}} = \max(0, (\sigma_{\text{out}} - \sigma_{\text{n}})), \quad (14)$$

$$B = \min(A_{\text{in}}, A_{\text{out}}), \quad (15)$$

$$\eta(i, j) = 1 - \left[\frac{B - \min(B)}{\max(B) - \min(B)} \right] \frac{1}{k}, \\ k = 1, 2, 3, \dots, \quad (16)$$

where σ_{n} , σ_{in} , and σ_{out} are the estimated noise standard variance, local standard variances of image non-boundary and boundary areas of the estimated image, respectively. The variance of the noise can be estimated from smooth areas of degraded image. The local standard variance of image boundary is calculated by zero-adding method commonly, but this method may bring obvious deviation. So we set a non-boundary area whose size is $(1 + P : M - P) \times (1 + Q : N - Q)$, and other image area is set as boundary area, as shown in Fig. 1.

The local standard variance in the whole estimated image \hat{f} including the non-boundary and boundary areas can be calculated using a $(2P + 1) \times (2Q + 1)$ region centered at pixel (i, j) by

$$\sigma_{\text{n}}(\hat{f}(i, j)) = \left\{ \frac{1}{(2P + 1)(2Q + 1)} \sum_{k=i-P}^{i+P} \sum_{l=j-Q}^{j+Q} \left[\hat{f}(i, j) - M(\hat{f}(k, l)) \right]^2 \right\}^{\frac{1}{2}}, \quad (17)$$

where $\hat{f}(i, j)$ is the pixel gray value of the estimated image \hat{f} , and $M[\hat{f}(i, j)]$ is the local mean obtained by

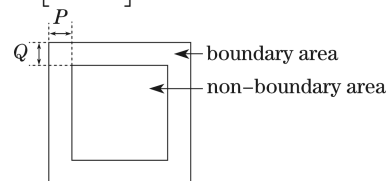


Fig. 1. Image non-boundary and boundary areas.

$$M(\hat{f}(k, l)) = \frac{1}{(2P+1)(2Q+1)} \times \sum_{k=i-P}^{i+P} \sum_{l=j-Q}^{j+Q} \hat{f}(k, l). \quad (18)$$

In the mixed-norm model, b_i changes along with the network state. And the modified updating rule is presented below.

{ For $i = 1 : 1 : L$

$$u_i = b_i(t) + \sum_{j=1}^L w_{ij} f_j(t)$$

$$\Delta \hat{f}_i = \begin{cases} 1 & u_i > \theta_i \\ 0 & -\theta_i < u_i < \theta_i \\ -1 & u_i < -\theta_i \end{cases},$$

where $\theta_i = -\frac{1}{2}w_{ii}$

$$\hat{f}_i(t+1) = K(\hat{f}_i(t) + \Delta \hat{f}_i),$$

$$\text{where } K(u) = \begin{cases} 0 & u < 0 \\ u & 0 \leq u \leq S \\ S & u > S \end{cases}$$

$t = t + 1$

End }

$$\Delta E_1 = -\frac{1}{2} \sum_{i=1}^L w_{ii} (\Delta \hat{f}_i)^2 - \sum_{i=1}^L u_i \Delta \hat{f}_i.$$

According to Eq. (12), calculate $b_i(t+1)$ and $\Delta E_2 = -\sum_{i=1}^L b_i(t+1) \hat{f}_i + \sum_{i=1}^L b_i(t) \hat{f}_i$.

If $\Delta E_1 = 0$, it means $\Delta E_1 + \Delta E_2 = 0$ and the network energy is stable. The final restored image is formed.

If $\Delta E_1 + \Delta E_2 < 0$, $b_i(t+1)$ is given to $b_i(t)$, repeat{ }

If $\Delta E_1 + \Delta E_2 > 0$, keep $b_i(t)$, repeat{ }

Experiments are performed to compare the proposed algorithm with the traditional algorithm and total variation algorithm. To evaluate performance of the algorithms, the improvement in signal-to-noise ratio (ISNR) is defined as

$$\text{ISNR} = 10 \log_{10} \frac{\|g - f\|_2^2}{\|\hat{f} - f\|_2^2}, \quad (19)$$

where f , g , and \hat{f} are the original, degraded, and restored images, respectively. In our experiments, the original test images are blurred by a Gaussian PSF whose size is 5×5 with the standard variance of 2.0 and added Gaussian white noise with various signal-to-noise ratios (SNRs). The regularizing parameter λ is 0.1. The value of k in Eq. (16) is 2. The local standard variance of the image is estimated using a 3×3 window. In other words, P and Q are equal to 1. The restored results are shown in Figs. 2, 3 and Table 1.

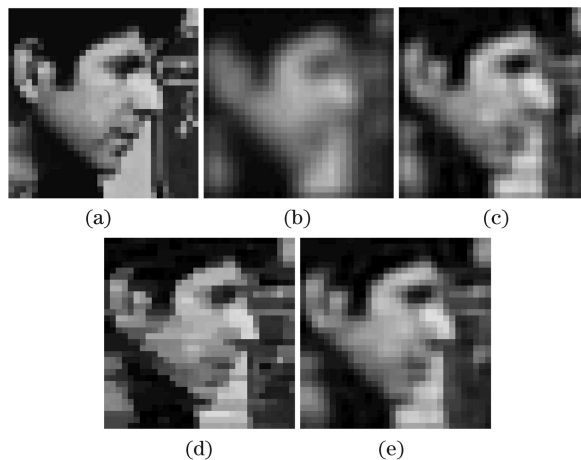


Fig. 2. Experimental results for cameraman's face (cropped to 32×32 for easier comparison). (a) Original image; (b) degraded image (SNR = 30 dB); (c) restored image using the traditional algorithm; (d) restored image using the total variation algorithm; (e) restored image using our algorithm.

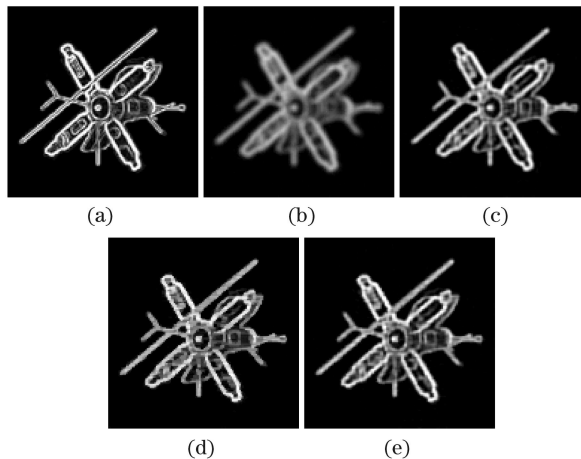


Fig. 3. Experimental results for satellite image. (a) Original image; (b) degraded image (SNR = 30 dB); (c) restored image using the traditional algorithm; (d) restored image using the total variation algorithm; (e) restored image using our algorithm.

Table 1. ISNRs of Restored Image Obtained by Different Algorithms

Image	SNR	Traditional	Total Variation	Our
Cameraman's	30 dB	4.1443	4.7966	5.2113
	Face	25 dB	3.6617	3.2812
Satellite	30 dB	4.1195	4.8273	5.2081
	25 dB	3.9665	4.2025	4.8208
Lena	30 dB	1.6650	2.0384	2.2313
	25 dB	1.3884	1.5893	1.7544
Peppers	30 dB	2.3946	2.9921	3.3441
	25 dB	2.0011	1.0984	2.6609

It is seen that our method works better than the method with a single norm. From Table 1, we can see that the ISNR using total variation in "Lena" image is quite close to the results obtained by the proposed method. This image has plenty of edge information such

as hat, hair, face, and so on. The total variation algorithm mainly preserves the image edges. And to some extent, the value selection of k in experiments affects the restoration effect using our algorithm. So the ISNR of total variation algorithm is close to that of our algorithm.

In conclusion, the algorithm proposed in this letter can remove noise and false edge in the smooth regions, preserve edge information, and prevent blur in the edge regions, and reduce ladder effect in slope edge regions. Experimental results demonstrate the effectiveness of the proposed algorithm. Still much improvement is possible, such as the parameters k , λ chosen adaptively, η chosen more exactly, and a faster updating rule. These will be further studied in the future.

This work was supported by the National Defense Pre-Research Foundation of China under Grant No. 9140A01040307HT0125.

References

1. C. Han, J. Li, X. Chen, and Z. Zhu, *Chin. Opt. Lett.* **6**, 334 (2008).
2. Z. Wang and Y. Tang, *Chin. Opt. Lett.* **6**, 405 (2008).
3. Q. Li, S. Liao, H. Wei, and M. Shen, *Chin. Opt. Lett.* **5**, 201 (2007).
4. J. K. Paik and A. K. Katsaggelos, *IEEE Trans. Image Processing* **1**, 49 (1992).
5. Y. Sun, *IEEE Trans. Signal Processing* **48**, 2105 (2000).
6. S. W. Perry and L. Guan, *IEEE Trans. Neural Networks* **11**, 156 (2000).
7. H.-S. Wong and L. Guan, *IEEE Trans. Neural Networks* **12**, 516 (2001).
8. E. Salari and S. Zhang, *Int. J. Imaging Syst. Technol.* **12**, 247 (2003).
9. E. Binaghi, I. Gallo, A. Guidali, M. Raspanti, and G. Salvini, in *Proceedings of International Machine Vision and Image Processing Conference* 207 (2007).
10. Y. Wang, X. He, and H. Wang, in *Proceedings of 3rd International Conference on Natural Computation* 363 (2007).
11. L. I. Rudin, S. Osher, and E. Fatemi, *Physica D* **60**, 259 (1992).
12. T. F. Chan and C.-K. Wong, *IEEE Trans. Image Processing* **7**, 370 (1998).
13. F. Malgouyres, *IEEE Trans. Image Processing* **11**, 1450 (2002).
14. Y.-D. Wu, Q.-X. Zhu, S.-X. Sun, and H.-Y. Zhang, *Neurocomputing* **69**, 2364 (2006).
15. L. V. Ferreira, E. Kaszkurewicz, and A. Bhaya, in *Proceedings of 2008 International Joint Conference on Neural Networks* 2512 (2008).
16. M. Zou, *Deconvolution and Signal Recovery* (National Defence Industry Press, Beijing, 2001).